Mon. Not. R. Astron. Soc. **271,** L10–L14 (1994)

The mass of the black hole in V 404 Cygni

T. Shahbaz,[1] F. A. Ringwald,[1*] J. C. Bunn,[2] T. Naylor,[1] P. A. Charles[2] and J. Casares[2]

[1] *Department of Physics, Keele University, Keele, Staffordshire ST5 5BG*
[2] *Department of Astrophysics, Nuclear Physics Laboratory, Keble Road, Oxford OX1 3RH*

Accepted 1994 August 22. Received 1994 August 10; in original form 1994 July 8

ABSTRACT

We have obtained a *K*-band infrared light curve of the low-mass X-ray binary transient V404 Cygni. We model it as the ellipsoidal variation of a secondary star distorted in the gravitational field of a black hole, and thus deduce the inclination of the binary. Combining this with previously published spectroscopic data, we determine the mass of the black hole to be approximately 12 $M_{\odot}$.

Key words: accretion, accretion discs – black hole physics – binaries: close – binaries: spectroscopic – stars: individual: V404 Cyg – X-rays: stars.

1 INTRODUCTION

The low-mass X-ray binary (LMXB) transients are systems where a late-type star is losing material via an accretion disc to a black hole or neutron star. The mass accretion on to the compact object is episodic, leading to outbursts which last for months, with a recurrence time of the order of decades. These systems are discovered by their X-ray emission during outburst, but, when they return to quiescence, detailed observations can be made of the secondary star. V404 Cyg has been typical of this pattern, being discovered by the *Ginga* All Sky Monitor (Makino et al. 1989), and with follow-up optical spectroscopy showing the period to be 6.5 d (Casares, Charles & Naylor 1992). Optical spectroscopy can provide a lower limit to the mass of the compact object (in this case 6.08 $M_{\odot}$) and thus provide support for the hypothesis that it is a black hole candidate. It can also yield the mass ratio, q, of the binary (Casares & Charles 1994); to obtain the mass of the compact object, however, requires a further measurement of the inclination (i) as a function of q. Just such information is provided by the ellipsoidal variation of the secondary star, i.e. the variation caused by observing the changing aspect of a gravitationally distorted star, which has been observed in the optical by Wagner et al. (1992). We have carried out such observations in the infrared K band, since here uncertainties in gravity- and limb-darkening parameters become negligible, and there appears to be little or no contribution from the accretion disc. Again V404 Cyg seems typical, with 84 per cent or more of the continuum flux close to Hα coming from the secondary star, a fraction which rises with increasing wavelength while the veiling ratio falls (see Casares et al. 1993, henceforth C^{2}NP). We have applied this technique to the neutron star system Cen X-4, where the result was consistent with the canonical neutron star mass (Shahbaz, Naylor & Charles 1993, henceforth SNC93); and to the black hole binary V616 Mon (= A0620 – 00), where the derived mass lay in the range 5 to 17 $M_{\odot}$ (Shahbaz, Naylor & Charles 1994, henceforth SNC94). In this paper we measure the mass of a second black hole, that in V404 Cyg.

*Visiting astronomer, Kitt Peak National Observatory, National Optical Astronomy Observatories.

2 OBSERVATIONS AND REDUCTION

We observed V404 Cyg in 1992 August and 1993 September using infrared array cameras on the 3.8-m United Kingdom Infrared Telescope (UKIRT), and in 1993 December on the Kitt Peak National Observatory (KPNO) 1.3-m telescope. The UKIRT array (IRCAM) is an InSb device, used at 0.62 arcsec per pixel. The KPNO imager is a HgCdTe array, which gives 1.96 arcsec per pixel on the 1.3-m telescope. The K-band filter used at UKIRT had a long-wavelength cut-off at 2.4 μm, whilst the KPNO K'-filter cut-off is at 2.3 μm. At both telescopes the images were taken in groups, using a slightly different telescope pointing position for each image. We observed the source for of the order of one hour per night, made up of a series of such groups.

The first step of the data reduction was to linearize the images, and then subtract the dark current. Next, a sky image was created for each data frame, by making a median-filtered image from all the other frames within the group. Each data frame was then flat-fielded using the appropriate sky image.

Aperture photometry of V404 Cyg is problematical because of a nearby (1.4 arcsec north) star. For the UKIRT data we therefore used a relatively large aperture (2.4 arcsec) which encompassed both stars, and then subtracted the contribution of the companion from all our measurements. This contribution was measured by using profile fitting (Stetson 1987) on frames with relatively good seeing. To check that variations in the seeing would not adversely affect such a procedure, we have carried out simulations (see C^2NP) which show that such an effect would not constitute an error of more than 0.7 per cent. For the Kitt Peak data, the large pixel size meant that the star 5.6 arcsec south of V404 Cyg would also contaminate an aperture containing V404 Cyg, so we reduced these data using the profile-fitting code.

Table 1. *K* measurements of V404 Cyg.

Heliocentric Julian Date	Phase	Telescope	K magnitude
2448856.859	0.6376-0.6431	UKIRT 1992	12.361 ± 0.051
2448858.001	0.8185-0.8195	UKIRT 1992	12.300 ± 0.017
2449233.787	0.8832 0.8919	UKIRT 1993	12.413 ± 0.003
2449234.796	0.0405-0.0475	UKIRT 1993	12.476 ± 0.004
2449235.811	0.1899-0.2109	UKIRT 1993	12.325 ± 0.002
2449235.943	0.2110 0.2306	UKIRT 1993	12.317 ± 0.002
2449236.775	0.3442-0.3546	UKIRT 1993	12.388 ± 0.004
2449237.745	0.4971-0.5035	UKIRT 1993	12.518 ± 0.002
2449238.841	0.6657-0.6717	UKIRT 1993	12.380 ± 0.004
2449324.631	0.9231-0.9277	Kitt Peak	12.471 ± 0.004
2449325.611	0.0747-0.0785	Kitt Peak	12.430 ± 0.006
2449326.605	0.2278-0.2326	Kitt Peak	12.240 ± 0.021
2449327.654	0.3921-0.3949	Kitt Peak	12.359 ± 0.014

To transform this light curve into apparent magnitude, we divided the counts obtained from V404 Cyg by those of two 'local standards' in each frame. Examination of field stars showed that the colour correction between the two photometric systems is significant, and so we applied a colour correction both to the comparison star, and to V404 Cyg. It should be noted, however, that V404 Cyg was the reddest star in the UKIRT field of view, and so the correction had to be extrapolated. This may lead to a colour-dependent error (see Section 3). Finally, we tied the magnitudes of the local standards to those of UKIRT standard stars, which adds a further systematic uncertainty of 0.004 mag to all the photometry.

The duration of each night's observation is so short that the expected variation during the night resulting from an ellipsoidal modulation of period 6.5 d is small (about half a per cent). Thus we binned the data points (748 from UKIRT and 151 from KPNO) into longer time-spans, to yield the light curve given in Table 1. Each data point was derived by fitting a histogram of the data values to a Gaussian distribution, and taking the resulting mean value. This removes points with a large deviation from the mean, which are caused by poorly corrected 'bad' pixels lying within either the target or the local standard star photometric aperture. The aperture photometry routine that we used (SNC94) gives a robust estimate of the errors. When the expected error falls to less than about 1 per cent per data frame, however, the observed scatter in the observations remains at about the

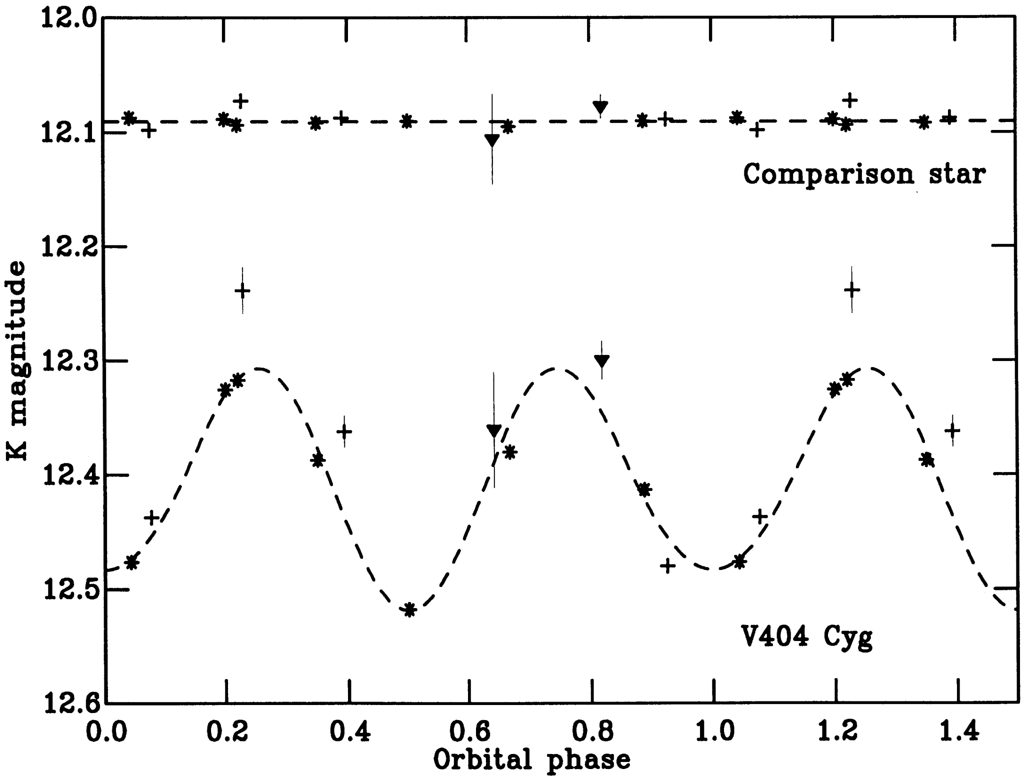

Figure 1. The *K*-band light curve of V404 Cyg, folded on the orbital phase with a comparison star shown above. The symbols indicate from which observing run the data are taken: stars – UKIRT 1993; triangles – UKIRT 1992; crosses – Kitt Peak. Where the error is larger than the symbol, an error bar is plotted as a thin line. The dashed curve is the best-fitting model light curve, and the dashed straight line a constant fitted to the comparison star.

1 per cent level, probably because of gaps between pixels (SNC93). Thus the errors given in Table 1 are standard errors calculated using the standard deviation within each time-bin. Finally, the data were folded on the ephemeris given by Casares & Charles (1994), to produce an orbital light curve (Fig. 1).

We have already presented limited IR photometry of V404 Cyg from 1990, about a year after outburst (C^{2}NP). These data were dominated by a modulation of 0.2-mag amplitude at a period of 5.9 h, which was also present in optical photometry and spectroscopy. The cause of this modulation is still unknown, but the data are consistent with it weakening in the years after outburst. To see whether this was still present in the IR, we obtained about 6 h of continuous coverage; the results are shown in Fig. 2, along with the overall ellipsoidal light curve from the fit to the entire data set. The data do not show any significant trends or flaring behaviour, any deviation from the expected light curve being less than 0.03 mag, and short-lived (less than about an hour). Our shorter runs on other nights are consistent with the same behaviour. We conclude, therefore, that the 6-h periodicity observed in earlier years is now either absent or much reduced in amplitude. Since V404 Cyg is now slightly fainter than it was in 1991 ($K=12.1$ to 12.4), this suggests that there was a variable contaminating component in 1991.

3 MODEL FITTING AND DERIVED PARAMETERS

We fitted the orbital light curve with an ellipsoidal model similar to that used for Cen X-4 and A0620−00 (SNC93; SNC94). The only difference is that, after calculating the temperature of each element of the secondary star surface, the flux is calculated by assuming a Kurucz solar-abundance model atmosphere with surface gravity $\log g=4.0$ (Kurucz 1991), rather than by assuming a blackbody. The free parameters were q and i, phase zero being fixed by the spectroscopic ephemeris, and the temperature of the secondary being taken as 4360 K, close to that derived by C^{2}NP, and consistent with the temperature derived in Section 4. The best fit gives $\chi^2_\nu=15.2$ at $q=5$, $i=62°$. Fitting of a constant magnitude to a comparison star reduced in an identical fashion to V404 Cyg gives $\chi^2_\nu=4.5$. That this value of χ^2_ν is not about unity suggests that there is a problem with the colour correction between the UKIRT and KPNO data. We therefore derived the errors for our fit by rescaling our error bars such that the best-fitting χ^2_ν was 1, and then choosing the 90 per cent confidence region to be $\chi^2+6.25$ (Lampton, Margon & Bowyer 1976). Fig. 3 shows the resulting allowed parameter space for V404 Cyg in the i–q plane. We also experimented by allowing the fitting procedure to add a contribution from a bright spot, and to shift phase zero with respect to the spectroscopic ephemeris. None of these experiments significantly affected the fit to the data, and none changed the derived inclination of the system by more than 0.4 per cent.

We can now combine the ellipsoidal study with a spectroscopic study to obtain the masses of the system's components in a similar manner to that described by SNC94. Using the values for the rotational broadening of $v \sin i=39.1$ km s^{-1} and the radial velocity semi-amplitude of $K_2=208.5$ km s^{-1} (Casares & Charles 1994), we obtain $q=16.7$. Constraining the (i, q) relationship obtained from the ellipsoidal study with this value of q, we find $i=56°$, which when combined with the value for the mass function allows us to obtain a complete solution for both masses, the orbital separation and

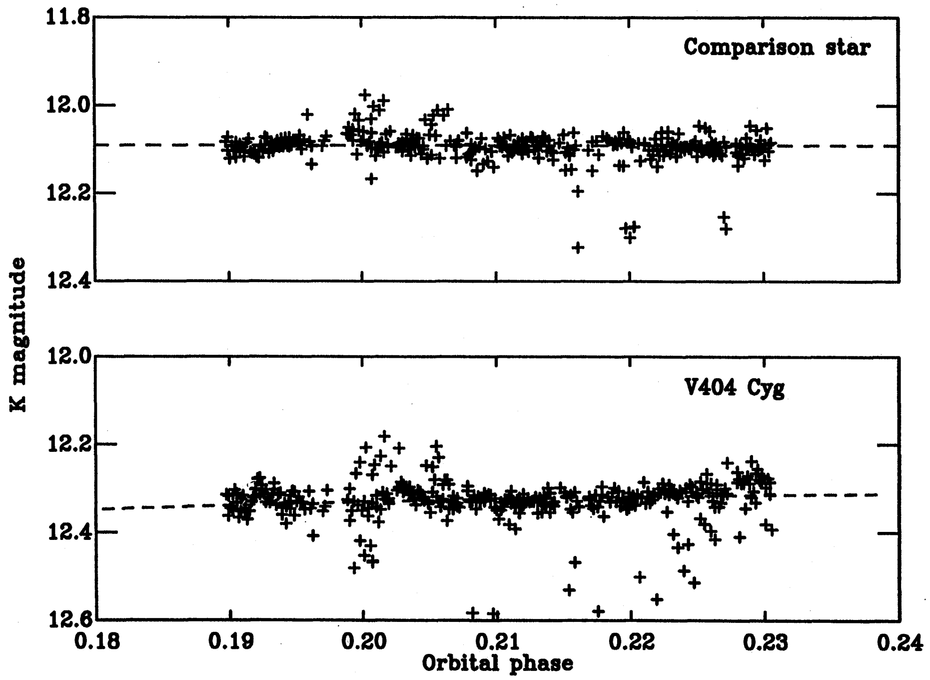

Figure 2. *K*-band light curves of V404 Cyg and a comparison star, lasting for about 6 h. The slow increase in flux is consistent with the ellipsoidal modulation, whose best-fitting light curve to the entire data set is shown as a dashed line. The few points with large deviations are caused by the target or local standard stars falling on a poorly corrected 'bad' pixel.

the radius of the secondary star. The latter two parameters are obtained using Kepler's Third Law and Paczyński's (1971) formula respectively. We present these in Table 2, along with their errors, derived using the Monte Carlo technique discussed by SNC94. Fig. 4 shows the allowed mass of the black hole as a function of secondary star mass.

4 DISCUSSION

The masses deduced for the black holes in both V404 Cyg (10–15 $M_\odot$) and V616 Mon (5–17 $M_\odot$: SNC94) are relatively large. The errors for V404 Cyg are sufficiently small that we can immediately rule out scenarios where the black hole is formed by the merger of neutron stars, provided only that they had masses of less than about 4 $M_\odot$ (the theoretical maximum mass for a maximally rotating neutron star – see Friedman & Ipser 1987).

High black hole masses present two problems for the classical scenarios of LMXB formation, where the initial binary is a low-mass (approximately 1 $M_\odot$) star in a wide orbit around the black hole progenitor. It is thought that supernova collapse into a neutron star produces a large velocity kick (e.g. Bailes 1989), which is likely to unbind the binary. If collapse to a black hole occurs with the same degree of asymmetry, its larger mass is even more likely to unbind the LMXB progenitor. Secondly, observations suggest that binaries with extreme mass ratios may be very

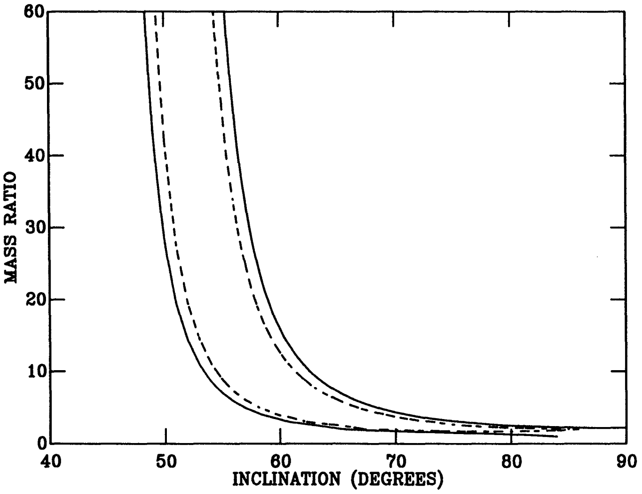

Figure 3. The 68 per cent (dashed line) and 90 per cent (solid line) confidence regions allowed for V404 Cyg in the inclination–mass ratio plane resulting from our fit to the ellipsoidal light curve.

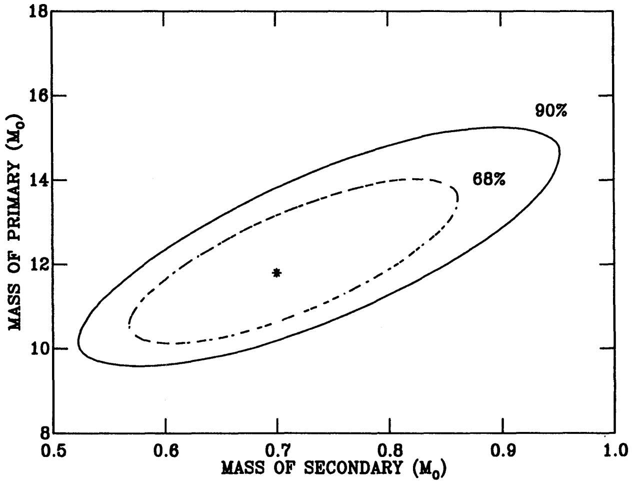

Figure 4. The 68 per cent (dashed line) and 90 per cent (solid line) confidence regions allowed for V404 Cyg in the M_2–M_1 plane resulting from combining our fit to the ellipsoidal light curve with the spectroscopic mass function and mass ratio.

Table 2. System parameters for V404 Cyg (with 90 per cent confidence regions derived using a Monte Carlo error propagation technique).

Parameter	Lower limit	Most likely value	Upper limit
Parameters derived from ellipsoidal study and spectroscopic data:			
Inclination i (degrees)	52	56	60
Primary mass M_1 ($M_\odot$)	10	12	15
Secondary mass M_2 ($M_\odot$)	0.5	0.7	1.0
Secondary radius R_2 ($R_\odot$)	5.5	6.0	6.7
Orbital separation a ($R_\odot$)	32	34	37
Assuming stripped giant model:			
Secondary core mass M_c ($M_\odot$)	0.213	0.216	0.221
Secondary luminosity L_2 ($L_\odot$)	10.18	10.20	10.23
Matching stripped giant luminosity to ellipsoidal model luminosity:			
Secondary effective temperature at pole (K)	4170	4355	4490
Mean secondary absolute magnitude M_V (mags)	3.3	3.4	3.6
Mean secondary absolute magnitude M_K (mags)	0.1	0.0	-0.1
Secondary predicted colour (V – K) (mags)	3.2	3.4	3.6
System distance D (kpc)	2.2		3.7
Visual extinction A_v (mags)	2.2		3.3

rare compared with those of more equal mass ratios (Halbwachs 1987). Both these effects will tend to make black hole LMXBs rare compared with, say, the bright bulge sources. In fact, the opposite seems to be the case, the relative proximity of the known black hole LMXBs compared with the neutron star LMXBs suggesting that the former may be more numerous (but see the discussion by van den Heuvel 1992). Neither problem is insurmountable, as there may be problems with observational selection in our statistics for binary mass ratios (Halbwachs 1987), and further investigations are needed into the velocity kick imparted during collapse into a black hole. It is interesting to note, though, that evolution via a Thorne–Żytkow object, as suggested by Podsiadlowski, Cannon & Rees (1994), would not suffer from such problems.

Using the value for the mass of the compact object, an upper limit to the distance can be obtained by assuming that the observed peak X-ray luminosity was Eddington-limited. Using an observed peak X-ray luminosity of $L_{\rm peak} = 1.4 \times 10^{38}\ D^2_{\rm kpc}$ erg s^{-1} (Tanaka 1989) and our upper limit for M_1, we obtain a 90 per cent upper limit to the distance of $D_{\rm kpc} \leq 3.7$ kpc.

Our solution for the radius of the secondary star can be used to make further predictions using the stripped giant models of Webbink, Rappaport & Savonije (1983), as suggested by King (1993). The radius of a stripped giant depends only on its core mass. Using the approximate equation for the radius given by King (1993), our radius implies a core mass of 0.216 $M_\odot$. The core mass that we obtain lies comfortably between the Schönberg–Chandrasekhar limit of 0.17 of the total mass of the secondary star (above which a stripped giant core must lie) and the total mass of the secondary star of about 0.7 $M_\odot$. This lends support to the evolutionary scenario for these systems where the mass transfer is driven by the expansion of the secondary star, which drives the system to longer orbital periods (e.g. SNC93; SNC94). The expansion can be that of a main-sequence star, which may well be the case for A0620 − 00 (Mukai 1994); or that of a subgiant, as may be the case for Cen X-4 (SNC93); or that of a stripped giant, as in the case of V404 Cyg.

The stripped giant model also predicts the luminosity as a function of core mass. We find, using the approximate equation for the model luminosity (King 1993), $L_2 = 10.20$ $L_\odot$. We therefore adjusted the temperature of the pole of our model secondary until its luminosity matched that predicted for a stripped giant. Due to gravity-darkening effects, this temperature is significantly different from that predicted for a blackbody of the same radius. The same model can be used to predict absolute K and V magnitudes, and the colour of the secondary star (see Table 1). We can derive an upper limit to the reddening by comparing the model and observed colours. We thus obtain a 90 per cent confidence upper limit of $A_V \leq 3.3$ by assuming no accretion disc contamination in K, 0.1-mag contamination in V (i.e. $V = 18.5$: C^{2}NP) and $A_K/A_V = 0.112$ (Rieke & Lebofsky 1985). We can use the upper limits for the distance and reddening to obtain corresponding lower limits for the reddening and distance using the absolute magnitude (see Table 2) and the distance modulus formula.

5 CONCLUSIONS

We have presented an ellipsoidal study of V404 Cyg, which, when combined with spectroscopic data, allows us to obtain a complete solution for the binary parameters. The mass of the black hole is relatively large (12 $M_\odot$), which presents some difficulties for standard evolutionary models. The mass of the secondary star is consistent with it being a stripped giant, the evolution of which is driving mass transfer in the system.

ACKNOWLEDGMENTS

We thank PATT for enabling us to observe V404 Cyg at some point during each of six successive nights on UKIRT. JC acknowledges support by the Ministerio Español de Educación y Ciencia (MEC). The United Kingdom Infrared Telescope is operated by the Royal Observatories on behalf of the UK Particle Physics and Astronomy Research Council. The National Optical Astronomy Observatories are operated by the Association of Universities for Research in Astronomy, Inc. (AURA), under cooperative agreement with the National Science Foundation. The data reduction was carried out on the Keele Starlink node using the ARK software.

REFERENCES

Bailes M., 1989, ApJ, 342, 917
Bailey J., 1981, MNRAS, 219, 619
Casares J., Charles P. A., 1994, MNRAS, 271, L5 (this issue)
Casares J., Charles P. A., Naylor T., 1992, Nat, 355, 614
Casares J., Charles P. A., Naylor T., Pavlenko E. P., 1993, MNRAS, 265, 834 (C^{2}NP)
Friedman J. L., Ipser J. R., 1987, ApJ, 314, 594
Halbwachs J. L., 1987, A&A, 183, 234
King A. R., 1993, MNRAS, 260, L5
Kurucz R. L., 1991, in Davis Philip, Upgren, Janes, eds, Van Vleck Obs. Contrib. No. 11, Precision Photometry Astrophysics of the Galaxy. L. Davis Press, Schenectady, NY
Lampton M., Margon B., Bowyer S., 1976, ApJ, 208, 177
Makino F. & the *Ginga* Team, 1989, IAU Circ. 4782
Mukai K., 1994, in Holt S. S., Day C., eds, AIP Conf. Proc. 308, The Evolution of X-ray Binaries. AIP, New York, p. 79
Paczyński B. E., 1971, ARA&A, 9, 183
Podsiadlowski Ph., Cannon R. C., Rees M. J., 1994, in Holt S. S., Day C., eds, AIP Conf. Proc. 308, The Evolution of X-ray Binaries. AIP, New York, p. 403
Rieke G. H., Lebofsky M. J., 1985, ApJ, 288, 618
Shahbaz T., Naylor T., Charles P. A., 1993, MNRAS, 265, 655 (SNC93)
Shahbaz T., Naylor T., Charles P. A., 1994, MNRAS, 268, 756 (SNC94)
Stetson P. B., 1987, PASP, 99, 191
Tanaka Y., 1989, in Hunt J., Battrick B., eds, Proc. 23rd ESLAB Symp. on Two Topics in X-ray Astronomy. ESA Publ. Division, SP-296, p. 1
van den Heuvel E. P. J., 1992, in Guyenne T. D., Hunt J. J., eds, Proc. Satellite Symp. 3: Space Sciences with particular emphasis on High-Energy Astrophysics. ESA ISY-3, p. 29
Wagner R. M., Kreidl T. J., Howell S. B., Starrfield S. G., 1992, ApJ, 401, L97
Webbink R. F., Rappaport S., Savonije J. G., 1983, ApJ, 270, 678